



## RESEARCH PAPER

# *Fam163a* knockdown and mitochondrial stress in the arcuate nucleus of hypothalamus reduce AgRP neuron activity and differentially regulate mitochondrial dynamics in mice

Cihan Suleyman Erdogan<sup>1</sup> | Yavuz Yavuz<sup>1,2</sup> | Huseyin Bugra Ozgun<sup>1</sup> |  
Volkan Adem Bilgin<sup>1</sup> | Sami Agus<sup>1,3</sup>  | Ugur Faruk Kalkan<sup>1</sup> | Bayram Yilmaz<sup>1,4,5</sup> 

<sup>1</sup>Department of Physiology, Faculty of Medicine, Yeditepe University, Istanbul, Turkey

<sup>2</sup>Department of Neuroscience and Pharmacology, The University of Iowa Carver College of Medicine, Iowa City, USA

<sup>3</sup>Department of Physiology, Augusta University, Augusta, Georgia, USA

<sup>4</sup>Department of Physiology, Faculty of Medicine, Dokuz Eylül University, Izmir, Turkey

<sup>5</sup>Izmir Biomedicine and Genome Center, Izmir, Turkey

## Correspondence

Bayram Yilmaz, Department of Physiology, Faculty of Medicine, Dokuz Eylül University, Izmir, Turkey.  
Email: [byilmaz@yeditepe.edu.tr](mailto:byilmaz@yeditepe.edu.tr)

## Funding information

Yeditepe University Research Projects and Scientific Activities Support Commission, Grant/Award Number: HD22006

## Abstract

**Aim:** Mitochondria play key roles in neuronal activity, particularly in modulating agouti-related protein (AgRP) and proopiomelanocortin (POMC) neurons in the arcuate nucleus of the hypothalamus (ARC), which regulates food intake. FAM163A, a newly identified protein, is suggested to be part of the mitochondrial proteome, though its functions remain largely unknown. This study aimed to investigate the effects of *Fam163a* knockdown and mitochondrial dysfunction on food intake, AgRP neuron activity, and mitochondrial function in the hypothalamus.

**Methods:** Male C57BL/6 and AgRP-Cre mice received intracranial injections of either *Fam163a* shRNA, rotenone, or appropriate controls. Behavioral assessments included food intake, locomotor activity, and anxiety-like behaviors. qRT-PCR was used to quantify the expression of the genes related to food intake, mitochondrial biogenesis, dynamics, and oxidative stress. Blood glucose, serum insulin, and leptin levels were measured. Electrophysiological patch-clamp recordings were used to assess the AgRP neuronal activity.

**Results:** *Fam163a* knockdown in the ARC increased the cumulative food intake in short term (first 7 days) without altering the 25-day food intake and significantly increased the *Pomc* mRNA expression. *Fam163a* silencing significantly reduced leptin levels. Both *Fam163a* knockdown and rotenone significantly reduced the firing frequency of AgRP neurons. Neither *Fam163a* silencing nor rotenone altered locomotor or anxiety-like behaviors. *Fam163a* knockdown and rotenone differentially altered the expression of mitochondrial biogenesis-, mitophagy-, fusion-, and oxidative stress-related genes.

**Conclusion:** Hypothalamic FAM163A may play a role in modulating AgRP neuronal activity through regulating mitochondrial biogenesis, dynamics, and redox

state. These findings provide insights into the role of FAM163A and mitochondrial stress in the central regulation of metabolism.

#### KEYWORDS

AgRP neurons, FAM163A, hypothalamus, mitochondria, rotenone

## 1 | INTRODUCTION

At the organismal level, energy homeostasis is regulated by the central nervous system (CNS) that adjusts energy intake and expenditure in response to internal metabolic changes.<sup>1</sup> The hypothalamus plays a key role in regulating energy homeostasis by integrating various neural and peripheral signals through specific neuronal populations located within multiple nuclei.<sup>2,3</sup> Among the neurocircuits, two distinct neuronal populations in the arcuate nucleus of the hypothalamus (ARC), orexigenic neurons co-express neuropeptide Y (NPY), and agouti-related peptide (AgRP) and anorexigenic neurons that express proopiomelanocortin (POMC), oppositely regulate food intake and energy expenditure.<sup>4</sup> Orexigenic signals, such as ghrelin, from peripheral tissues activate the AgRP neurons leading to the release of NPY and AgRP, as well as gamma-aminobutyric acid (GABA) and the induction of food intake.<sup>5–9</sup> In addition, anorexigenic signals, including insulin, glucagon-like peptide 1 (GLP-1), and leptin, inhibit the AgRP and activate the POMC neurons resulting in the reduction of food intake.<sup>10–15</sup>

Mitochondria are essential and complex organelles that enable adequate energy production through oxidative phosphorylation to maintain the biological reactions in eukaryotic cells. They are highly plastic and dynamic organelles that respond to different stress conditions and metabolic demands through the process of mitochondrial dynamics that includes fusion, fission, mitophagy, and transport processes within the cells.<sup>16</sup> Mitochondrial biogenesis, a related but distinct process from the mitochondrial dynamics, also contributes to the energy needs of the cell.<sup>16</sup> Due to the high energy demand for synaptic functions and electrical excitability, mitochondria are pivotal for neuronal health, development, and function.<sup>17–19</sup> Previous studies indicated that hypothalamic mitochondria play a role in the modulation of energy balance through mitochondrial dynamics and modulate the activities of AgRP and POMC neurons.<sup>20,21</sup> In orexigenic AgRP neurons, mitochondrial fission is observed under negative energy balance conditions, while in positive energy balance conditions such as a high-fat diet, mitochondrial density, and area are increased, indicating mitochondrial fusion.<sup>20,22</sup> However, under satiety conditions,

mitochondrial fission is observed in POMC neurons and that was suggested to be associated with increased hypothalamic oxidative stress.<sup>23</sup>

Rotenone, a potent mitochondrial complex I inhibitor, disrupts the mitochondria electron transport chain and increases the reactive oxygen species (ROS) production.<sup>24</sup> Previous literature indicated that appetite and satiety are affected by the reactive oxygen species in the ARC.<sup>25,26</sup>

FAM163A is a relatively newly discovered protein,<sup>27,28</sup> and its function and intracellular localization are not yet fully understood.<sup>27–34</sup> It was reported to be predominantly expressed in the brain of the mouse with higher expression in the postnatal period compared to the embryonic period.<sup>28</sup> It was previously discovered in the SH-SY5Y neuroblastoma cell line as a secreted protein<sup>27</sup> and reported to promote the proliferation of neuroblastoma cells.<sup>27,35</sup> Additionally, a previous proteomics study demonstrated that FAM163A is present in the mitochondrial proteome of SH-SY5Y cells,<sup>33</sup> suggesting its possible roles in mitochondrial dynamics and function.

In the present study, we aimed to investigate the effects of hypothalamic *Fam163a* knockdown (KD) and rotenone-induced mitochondrial damage on food intake, neurobehavioral parameters, and hypothalamic mitochondrial dynamics and biogenesis in mice. We also investigated the effect of *Fam163a* KD and rotenone-induced mitochondrial damage on the electrophysiological activity of AgRP neurons.

## 2 | RESULTS

### 2.1 | *Fam163a* knockdown, but not rotenone administration, increases cumulative food intake in short-term

Previously, FAM163A was suggested to be expressed in the brain.<sup>28</sup> Moreover, the Allen Brain Atlas and Bonthuis et al. reported the expression of *Fam163a* in the ARC of the mouse.<sup>36–38</sup> In our study, we confirmed FAM163A expression in the hypothalamus using immunofluorescence staining and qPCR. Our results showed that FAM163A is ubiquitously expressed in the ARC in mice (Figure 1A–C). Intracranial shRNA injection of *Fam163a*-shRNA into

## FAM163A / DAPI

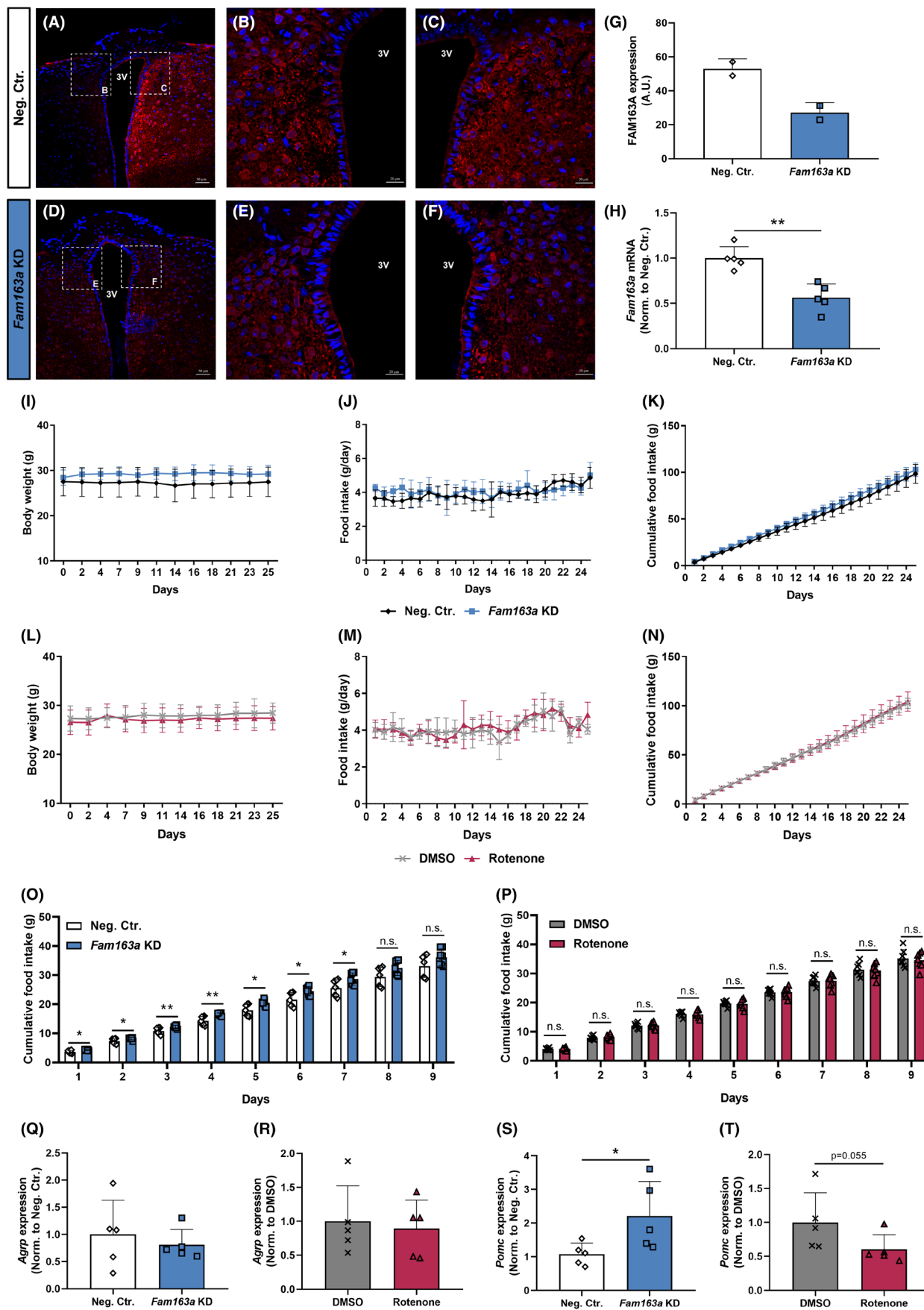


**FIGURE 1** *Fam163a* knockdown, but not rotenone administration, increases cumulative food intake in short term. (A–H) Validation of shRNA-mediated knockdown of *Fam163a* in the ARC by (A–G) immunostaining against FAM163A (Scale bars: A and D, 50  $\mu$ m and B, C, E, and F, 20  $\mu$ m) and (H) qPCR. (I and L) Body weight measurements ( $n = 7$  mice for all groups). (J, K, M and N) Daily and cumulative food intake measurements during the 25-day period ( $n = 7$  mice for all groups). (O and P) Cumulative food intake measurements during the first 9 days ( $n = 7$  mice for all groups). (Q–T) qPCR analysis of hypothalamic *Agrp* and *Pomc* mRNA levels ( $n = 5$  mice for all groups) (Statistical analysis: Student's unpaired *t*-test; \* $p < 0.05$  and \*\* $p < 0.01$ ; 3V, third ventricle).

the ARC resulted in a ~50% reduction in both FAM163A protein (Figure 1A–G) and *Fam163a* mRNA levels (Figure 1H;  $p < 0.01$ ).

Next, we investigated whether *Fam16a* knockdown or rotenone administration in the ARC influences body weight and food intake. Body weight and daily food intake of the animals were similar in *Fam163a* KD and rotenone-administered animals compared to their control groups (Neg. Ctr. and DMSO groups, respectively; Figure 1I,J,L,M). Similarly, the cumulative food intake of *Fam163a* KD and rotenone groups were similar to their respective control groups at the end of the 25-day period (Figure 1K,N). Interestingly, cumulative food intake was significantly higher in of *Fam163a* KD group compared with the Neg. Ctr. group during the first 7 days, while this difference disappeared thereafter (Figure 1K,O,  $p < 0.05$ ). Nevertheless, cumulative food intake of the DMSO and rotenone groups was similar throughout the experimental period (Figure 1N,P).

As the AgRP and POMC neurons are the two key neuronal populations regulating food consumption,<sup>4</sup> we investigated the levels of *Agrp* and *Pomc* mRNA in the hypothalamus. *Agrp* levels were not altered by either *Fam163a* knockdown or rotenone administration (Figure 1Q,R). However, *Fam163a* knockdown led to a significant increase in *Pomc* levels (Figure 1S,  $p < 0.05$ ), while rotenone administration tended to decrease the *Pomc* levels in the hypothalamus (Figure 1T,  $p = 0.055$ ).

## 2.2 | *Fam163a* knockdown negatively regulates serum leptin levels

Since blood glucose, serum insulin, and leptin levels are regulated by the neurons located in the ARC,<sup>39–41</sup> we investigated the effect of *Fam163a* silencing and mitochondrial stress on these parameters. Blood glucose and serum insulin levels were not altered by either *Fam163a* silencing (Figure 2A,B) or rotenone administration (Figure 2D,E). Serum leptin levels of the animals in the *Fam163a* KD group, however, were found to be significantly lower compared to the Neg. Ctr. group (Figure 2C), while serum leptin levels were not altered by rotenone administration (Figure 2F).

## 2.3 | *Fam163a* knockdown and rotenone administration decrease the firing rate of ARC<sup>AgRP</sup> neurons

Next, we investigated the electrophysiological response of the ARC<sup>AgRP</sup> neurons upon *Fam163a* silencing or mitochondrial stress caused by rotenone. First, we validated that ARC<sup>AgRP</sup> neurons express FAM163A by immunofluorescence imaging (Figure 3A–D). To record the neuronal activity, we ensured proper attachment to the neurons expressing GFP (Figure 3E). In response to *Fam163a* knockdown, the firing frequency of AgRP neurons was significantly reduced ( $p < 0.05$ ; Figure 3F,G). Similarly, rotenone administration led to a reduction in the firing frequency of AgRP neurons ( $p < 0.01$ ; Figure 3H,I).

## 2.4 | Neither *Fam163a* knockdown nor rotenone significantly alters locomotor activity and anxiety-like behavior

As the neurons located in the ARC are implicated in regulating locomotor activity<sup>42–44</sup> and stress responses,<sup>45,46</sup> we investigated the behavioral effects of the *Fam163a* knockdown and mitochondrial stress. *Fam163a* knockdown did not alter the total distance traveled and average velocity (Figure 4A,B), while it tended to increase the time spent in the center area in the OFT ( $p = 0.067$ ; Figure 4C). On the other hand, rotenone administration tended to decrease the total distance traveled and average velocity ( $p = 0.066$ ; Figure 4D,E), while significantly increasing the time spent in the center area ( $p < 0.05$ ; Figure 4F).

In the EPM test, *Fam163a* knockdown did not alter the total distance traveled, average velocity, number of arm entries, and time spent in the arms (Figure 5A,C,E,G,I,K and Figure S1). Although not being significantly altered, total distance traveled (Figure 5B), average velocity (Figure 5D), time spent in open arms (Figure 5H and Figure S1) and number of closed arm entries (Figure 5J) tended to decrease, while the time spent in closed arms had a tendency to increase in the rotenone group (Figure 5L and Figure S1). On the other hand, neither *Fam163a*



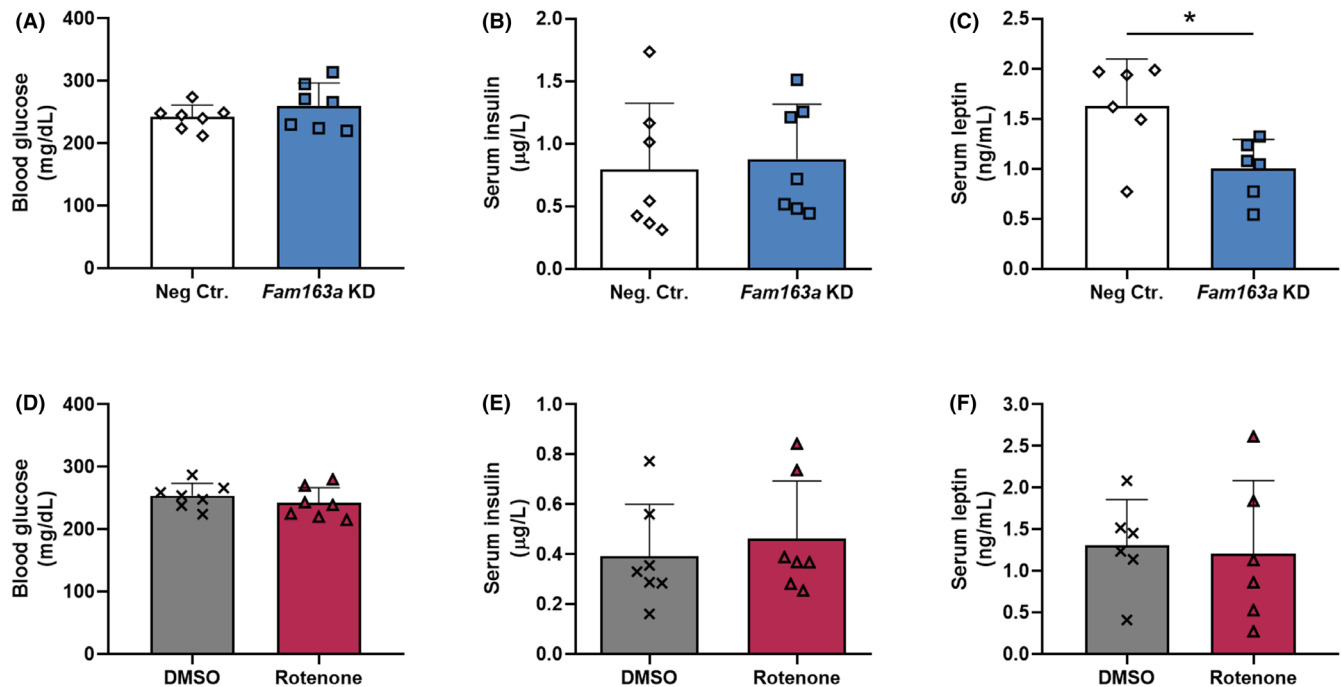


**FIGURE 2** *Fam163a* knockdown negatively regulates serum leptin levels. (A and D) Blood glucose levels ( $n=7$  mice for all groups). (B and E) Serum insulin levels ( $n=7$  mice for all groups). (C and F) Serum leptin levels ( $n=6$  mice for all groups). (Statistical analysis: Student's unpaired  $t$ -test; \* $p=0.018$ ).

knockdown nor rotenone treatment alters the time spent in the center area (Figure 5M,N and Figure S1).

## 2.5 | *Fam163a* knockdown and mitochondrial stress differentially regulate mitochondrial dynamics

A previous study reported that *Fam163a* was found in the mitochondrial proteome of the SH-SY5Y neuroblastoma cell line.<sup>33</sup> Moreover, rotenone, a well-known inhibitor of mitochondrial complex I in the electron transport chain, causes mitochondrial dysfunction and neuronal cell death.<sup>47,48</sup> Therefore, we investigated the effects of *Fam163a* knockdown and rotenone administration on the mitochondrial biogenesis- and dynamics-related, as well as oxidative stress-related genes in the hypothalamus.

PGC-1 $\alpha$ , PGC-1 $\beta$ , NRF1, NRF2, TFAM, and ERR $\alpha$  are among the key mitochondrial biogenesis-related factors that are essential for proper neuronal functionality and health.<sup>49–51</sup> *Pgc-1a* and *Pgc-1b* were not significantly altered by either *Fam163a* knockdown or rotenone treatment in the hypothalamus (Figure 6A). However, we observed a tendency to increase and decrease in the *Pgc-1b* mRNA expression in the *Fam163a* KD and rotenone groups, respectively ( $p=0.076$  and  $p=0.053$ , respectively; Figure 6A). *Nrf1* mRNA levels were similar in the *Fam163a* KD and

rotenone groups compared to the respective control groups (Figure 6A). However, while *Nrf2* mRNA levels were not altered in the *Fam163a* KD group ( $p=0.062$ , Figure 6A), rotenone administration significantly reduced *Nrf2* mRNA levels in the hypothalamus ( $p=0.013$ ; Figure 6A). *Tfam* mRNA levels were downregulated by both *Fam163a* silencing and rotenone treatment ( $p=0.043$  and  $p=0.007$ , respectively; Figure 6A). *Erra* mRNA expression, however, did not change either by *Fam163a* silencing or rotenone administration (Figure 6A).

Next, we investigated the levels of mitophagy-related genes in the hypothalamus of *Fam163a* KD and rotenone-treated animals. *Map1lc3a* mRNA expression was significantly reduced in the *Fam163a* KD group compared to the Neg. Ctr. ( $p=0.014$ ; Figure 6B), while rotenone did not alter the mRNA level of *Map1lc3a* (Figure 6B). While *Pink1* mRNA levels were found to be similar in both the *Fam163a* KD and rotenone groups compared to their respective control groups (Figure 6B), *Parkin* was significantly upregulated in the *Fam163a* KD group ( $p=0.034$ ; Figure 6B) and remained unchanged after rotenone treatment (Figure 6B). *P62* expression was significantly decreased in the *Fam163a* KD group ( $p=0.011$ ; Figure 6B) but it was similar in the rotenone and DMSO groups (Figure 6B). *Optn* mRNA levels were significantly higher in the *Fam163a* group compared to the Neg. Ctr. group ( $p=0.016$ ; Figure 6B) but not significantly altered by rotenone administration (Figure 6B). On the other

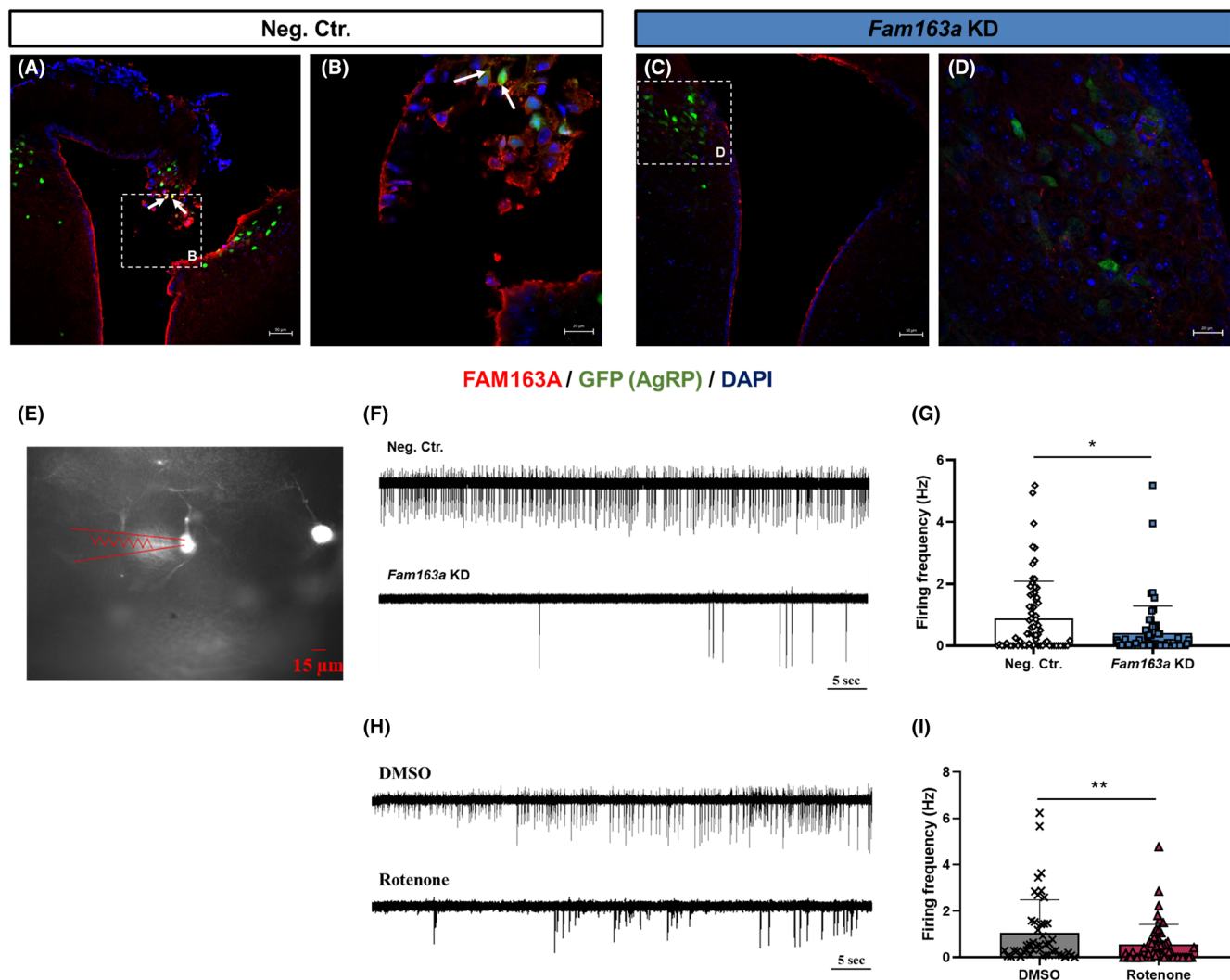


**FIGURE 3** *Fam163a* knockdown and rotenone reduce the firing rate of *ARC<sup>AgRP</sup>* neurons. (A and D) Representative immunostaining against FAM163A. White arrows depict the co-expression of GFP and FAM163A (Scale bars: [A and C] 50  $\mu$ m and [B and D] 20  $\mu$ m). (E) GFP expression in *AgRP* neurons containing brain slice of *AgRP*-Cre mouse. (Representative image depicting Cell-attached loose-seal recording from an *AgRP* neuron; recording pipette is highlighted with red-dashed lines, Scale bar: 15  $\mu$ m). (F and H) Representative loose-seal recording traces for each group. (G) Effect of *Fam163a* KD on firing rate of *AgRP* neurons ( $n = 3-4$  mice for each group; Neg. Ctr.  $n = 70$  neurons, *Fam163a* KD  $n = 63$  neurons) (I) Effect of rotenone on firing rate of *AgRP* neurons ( $n = 3-4$  mice for each group; DMSO  $n = 46$  neurons, rotenone  $n = 52$  neurons) (Data are mean  $\pm$  standard deviation. Statistical analysis: Mann-Whitney  $U$  test; \* $p = 0.017$ ; \*\* $p = 0.0062$ ).

hand, *Ndp52* and *Bnip3* mRNA levels were similar in the Neg. Ctr. and *Fam163a* KD groups, while rotenone treatment significantly reduced their expression in the hypothalamus compared to the DMSO group ( $p = 0.033$  and  $p = 0.046$ , respectively; Figure 6B). *Fundc1* mRNA levels were not altered either by *Fam163a* knockdown or rotenone administration.

Mitochondrial fusion has been implicated in regulating the *AgRP* neuron activity,<sup>20</sup> therefore, we also investigated the levels of the mitochondrial fusion genes in the hypothalamus. *Mfn1* and *Mfn2* mRNA levels were not altered, whereas *Opa1* mRNA levels were significantly reduced by *Fam163a* knockdown ( $p = 0.046$ ; Figure 6C). Interestingly,

*Mfn1* and *Opa1* mRNA levels were significantly upregulated in the rotenone group ( $p = 0.035$  and  $p = 0.025$ , respectively; Figure 6C).

Elevated ROS levels were reported to regulate *AgRP*/NPY and POMC activity.<sup>23,52,53</sup> In our study, *Fam163a* knockdown led to a significant decrease in *Ucp2* and *Hif-1a* levels ( $p = 0.006$  and  $p = 0.031$ , respectively), while there was a significant increase in the *Keap1* and *Ho-1* levels ( $p = 0.021$  and  $p = 0.015$ , respectively; Figure 6D). On the other hand, while *Ucp2*, *Ho-1*, and *Hif-1a* levels were not significantly altered in the rotenone group compared to the DMSO group, *Keap1* levels were significantly upregulated ( $p = 0.038$ ; Figure 6D).

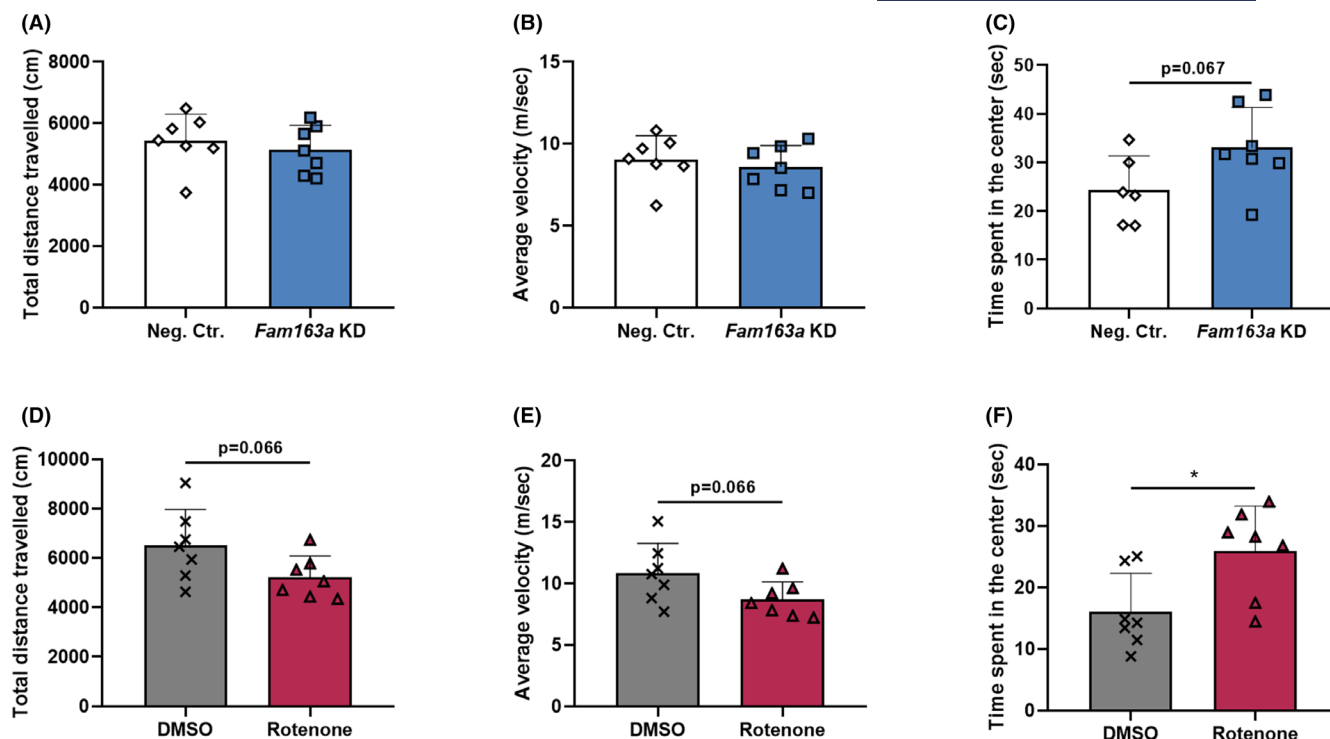


**FIGURE 4** *Fam163a* knockdown and rotenone do not alter the locomotor activity in OFT. (A and D) Total distance traveled ( $n=7$  mice for all groups), (B and E) average velocity ( $n=7$  mice for all groups), and (C and F) total time spent in the center ( $n=6$  for Neg. Ctr. and  $n=7$  mice for other groups). (Data are mean  $\pm$  standard deviation. Statistical analysis: (A, B and D–F) Student's unpaired  $t$ -test, (C) Mann–Whitney  $U$  test. \* $p=0.018$ ).

### 3 | DISCUSSION

Hypothalamic mitochondrial function is critical in various types of neurons that control energy homeostasis<sup>54</sup> and mitochondrial dysfunction occurring in hypothalamic neurons can contribute to the development of various metabolic diseases such as obesity and type 2 diabetes.<sup>55</sup> Mitochondrial proteome studies revealed that the majority of the proteins in the mitochondria are encoded by nuclear genes, translated in the cytoplasm, and imported into mitochondria.<sup>56</sup> The discovery that FAM163A, encoded by a nuclear gene, is expressed in the brain<sup>28</sup> and included in the mitochondrial proteome<sup>33</sup> led us to suggest that it may play a role in mitochondrial function and health, thereby affecting organismal energy metabolism. Our results showed that *Fam163a* silencing increased cumulative food intake in the short term, reduced AgRP neuron activity, and altered the expression of genes regulating mitochondrial dynamics. Additionally, mitochondrial dysfunction caused by rotenone led to a decrease in AgRP neuron firing frequency and changes in the expression of genes involved in mitochondrial dynamics and biogenesis without causing any differences in food intake.

Mitochondrial function and dynamics play a significant role in regulating the activity of AgRP and POMC neurons; thus, in the regulation of food intake.<sup>57</sup> The dynamic feature

of the mitochondria allows them to adapt to the energetic changes in the environment.<sup>20,21</sup> Mitochondrial fusion in AgRP neurons and fission in POMC neurons are observed during positive energy balance to maintain sustained neuronal activity and maximize energy uptake.<sup>20,57,58</sup> In our study, we observed that hypothalamic silencing of *Fam163a* increased cumulative food intake in the short term but not in the long term, while rotenone treatment did not alter food intake at any period. Additionally, we identified changes in the expression of genes regulating mitochondrial biogenesis, fusion, mitophagy, and oxidative stress either after *Fam163a* silencing or rotenone administration. Previously, it was reported that mice lacking *Mfn1* and *Mfn2* exhibited increased AgRP neuron activity and food intake.<sup>20</sup> In the deficiency of *Mfn2* in POMC neurons, on the other hand, POMC neuronal excitability is reduced and ER stress is increased.<sup>21</sup> On the other hand, POMC<sup>*Mfn1*−/−</sup> mice exhibited abnormalities in mitochondrial structure and decreased glucose sensitivity.<sup>59</sup> In the present study, *Fam163a* silencing resulted in nearly significant downregulation of *Mfn1* expression, significant downregulation of *Opa1* levels, and unaltered *Mfn2* expression. OPA1 deficiency in POMC neurons was reported to alter cristae structure and impair lipolysis.<sup>60</sup> Deletion of *Mfn1* in mice leads to impaired mitochondrial fusion and results in embryonic lethality during development.<sup>61</sup> Like *Mfn1*, *Mfn2* also plays a role in fusion<sup>62</sup>

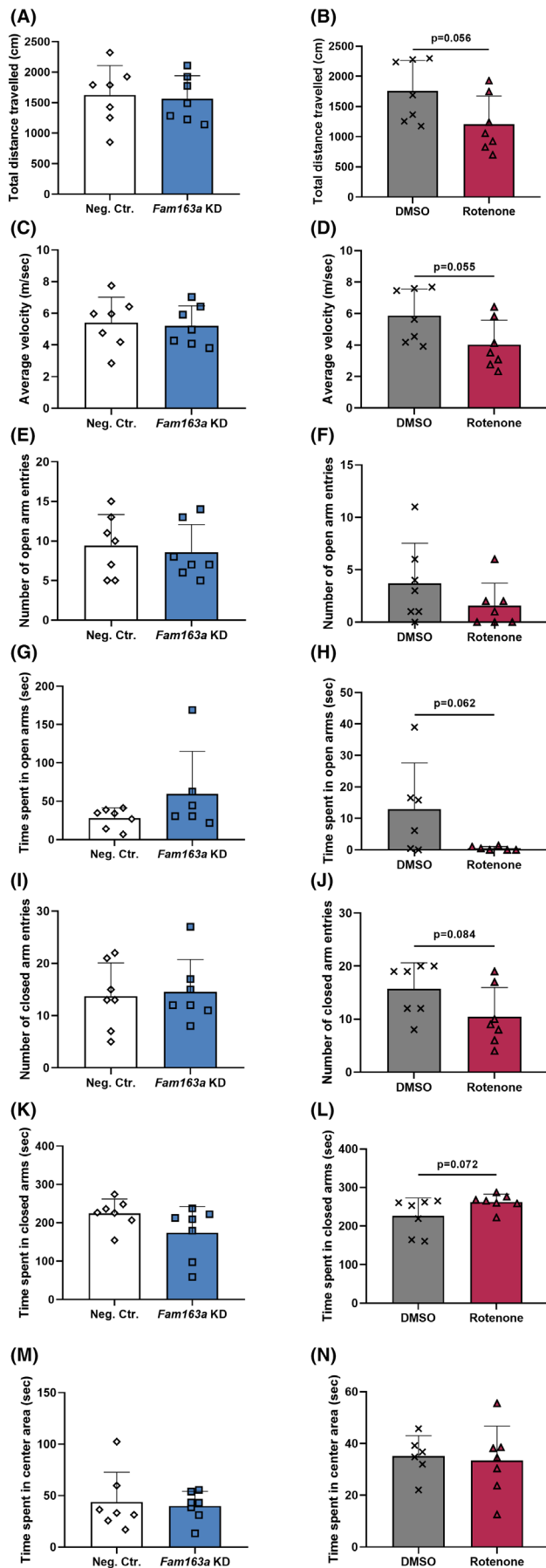


**FIGURE 5** *Fam163a* KD and rotenone do not alter the locomotor activity and anxiety-like behavior in EPM. (A and B) Total distance traveled ( $n=7$  mice for all groups), (C and D) average velocity ( $n=7$  mice for all groups), (E and F) number of open arm entries ( $n=7$  mice for all groups), (G and H) time spent in open arms ( $n=7$  mice for Neg. Ctr. and  $n=6$  for other groups), (I and J) number of closed arm entries ( $n=7$  mice for all groups), (K and L) time spent in open arms ( $n=7$  mice for all groups), and (M and N) time spent in the center area ( $n=6$  for DMSO and  $n=7$  mice for other groups). (Data are mean  $\pm$  standard deviation. Statistical analysis: (A–F and I–N) Student's unpaired *t*-test, (G and H) Mann–Whitney *U* test).

and is crucial for the connection between the ER and mitochondria, which is important for lipid exchange and mitochondrial calcium uptake between these two organelles.<sup>63,64</sup> The significantly decreased expression of *Opa1* and reduced *Mfn1* expression following *Fam163a* knockdown in the ARC suggests a state where mitochondrial fusion and function are compromised but not completely disrupted. Additionally, the transcription of *Mfn2* is enhanced by the physical interaction of PGC-1 $\alpha$  and PGC-1 $\beta$  with ERR $\alpha$ , which are key proteins in mitochondrial biogenesis.<sup>65,66</sup> The absence of differences in the expression of *Pgc-1 $\alpha$* , *Pgc-1 $\beta$* , and *ERR $\alpha$*  may explain the reason why *Mfn2* expression was found to be similar in both groups. Moreover, previous studies reported impaired fusion in response to the rotenone treatment in vitro<sup>67,68</sup> and in vivo.<sup>69</sup> In contrast, a significant increase in *Mfn1* and *Opa1* expression was detected 25 days after rotenone exposure observed in our study. As mitochondrial fusion acts as a repair mechanism for the damaged to compensate for the diminished mitochondrial energy production subsequent to the removal of damaged mitochondria,<sup>70</sup> the increased levels of fusion-related genes found in our study may be an attempt to repair the rotenone-induced mitochondrial damage.

In our study, *Tfam* levels were downregulated by *Fam163a* silencing. *Mfn1* and *Mfn2* maintain the expression of *Tfam*, the primary transcription factor responsible for regulating mtDNA copy number and mitochondrial mtRNA levels.<sup>71</sup> Studies have demonstrated that the simultaneous deletion of *Mfn1* and *Mfn2* in  $\beta$ -cells results in a significant reduction in *Tfam* expression, while the single deletion of both genes does not significantly alter it.<sup>71</sup> Additionally, *Tfam* and *Nrf2* expressions are reduced following rotenone exposure. In a rotenone-induced Parkinson's disease (PD) model, significant reductions were observed in the protein levels of PGC-1 $\alpha$ , NRF-1, and TFAM.<sup>72</sup> Another study revealed reduced NRF2 protein levels in an in vivo PD model.<sup>73</sup> NRF2 is not only a factor regulating mitochondrial biogenesis but also an important factor in the regulation of the oxidative stress response.<sup>74</sup> It also regulates the expression of various



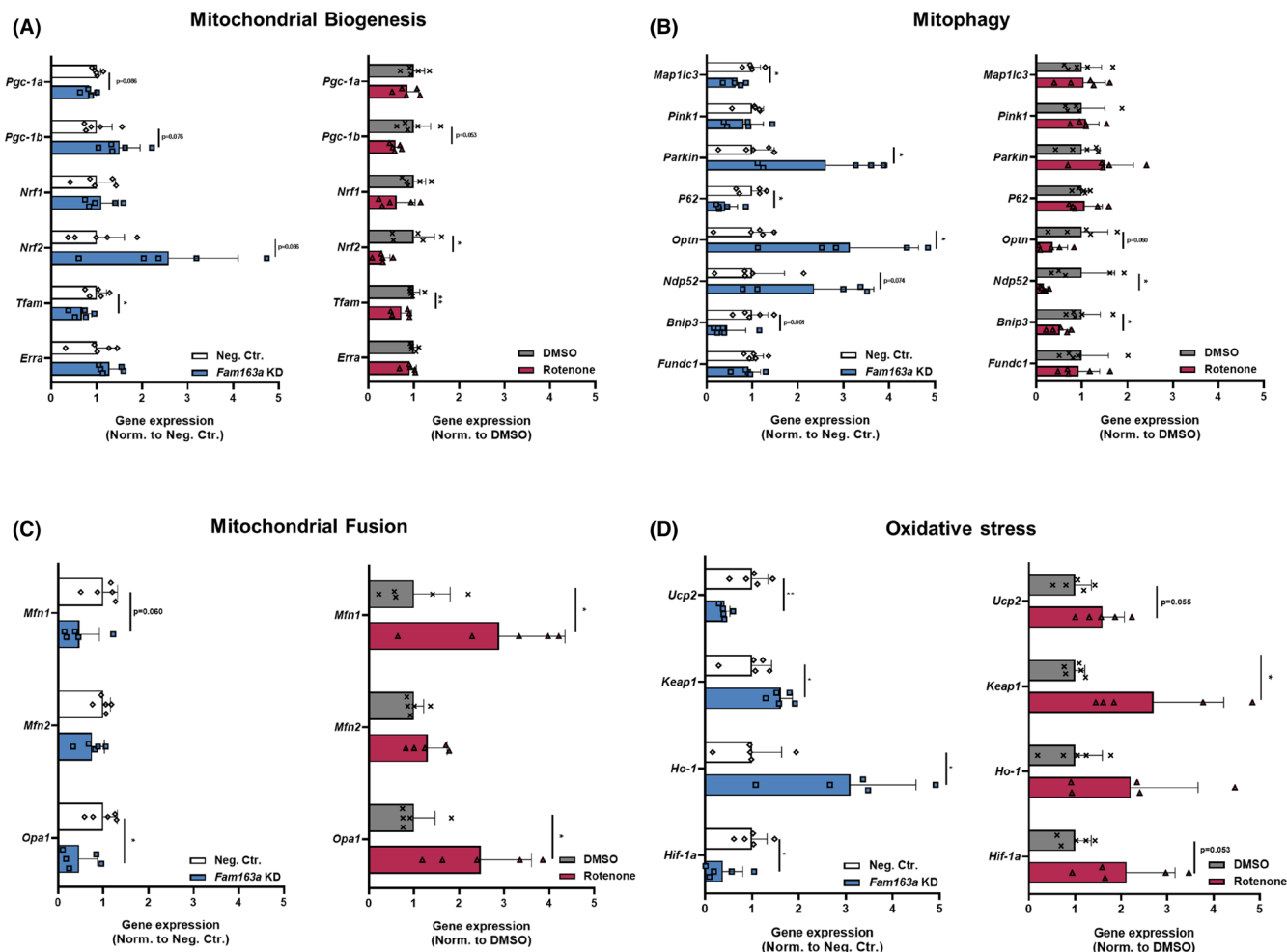


**FIGURE 6** *Fam163a* knockdown and mitochondrial stress differentially regulate mitochondrial dynamics. (A) mRNA expression of mitochondrial biogenesis-related genes, (B) mRNA expression of mitophagy-related genes, (C) mRNA expression of mitochondrial fusion genes, and (D) mRNA expression of oxidative stress-related genes (Data are mean  $\pm$  standard deviation.  $n = 5$  mice for all groups. Statistical analysis: Student's unpaired *t*-test or Mann-Whitney *U* test. \* $p < 0.05$  and \*\* $p < 0.01$ ).

protective proteins against oxidative stress, including HO-1.<sup>75</sup> Keap1, on the other hand, inhibits the activity of Nrf2<sup>76</sup> and increases the proteasomal degradation of Nrf2.<sup>77</sup> The increase in KEAP1 expression is expected to enhance the degradation of NRF2, thereby reducing the activation of ARE genes such as HO-1.<sup>78</sup> However, this is not always the case. One reason could be that, despite the increase in KEAP1 levels, the amount of NRF2 undergoing KEAP1-mediated degradation may remain constant due to the saturation of the KEAP1 degradation pathway.<sup>79</sup> Consequently, an increase in KEAP1 levels may not lead to a proportional decrease in NRF2 levels or HO-1 expression.<sup>79</sup>

Mitophagy, a type of macroautophagy, plays a vital role in neuronal survival, health, and function. Previous reports indicated that ROS induces mitophagy,<sup>80</sup> while chronic high-fat consumption impairs the mitophagy in the hypothalamus.<sup>81</sup> LC3 is involved in the formation and elongation of autophagosomes, the vesicles that sequester damaged organelles and proteins for degradation.<sup>82</sup>

PINK1 and PARKIN are proteins closely associated with mitochondrial quality control and cellular health, with mutations in the genes encoding these proteins linked to Parkinson's disease.<sup>83,84</sup> Generally, in a healthy cell, PINK1 is imported into healthy mitochondria and degraded, while PARKIN remains in the cytosol.<sup>85</sup> However, when a mitochondrion is damaged, the import of PINK1 is blocked, allowing it to accumulate on the outer mitochondrial membrane where PARKIN can localize.<sup>84</sup> PARKIN, an E3 ubiquitin ligase, then tags the damaged mitochondrion for degradation through a process known as PINK1/PARKIN-mediated mitophagy.<sup>84</sup> Polyubiquitinated mitochondrial proteins are identified by the autophagy cargo receptors p62/SQSTM1, OPTN, and NDP52, resulting in the sequestration of damaged mitochondria.<sup>86,87</sup> BNIP3 plays a significant role in hypoxia-induced mitophagy and plays a role in the selective removal of damaged mitochondria by promoting their recognition and engulfment by autophagosomes.<sup>88,89</sup> The observed gene expression

changes in our study indicate a complex response to *Fam163a* silencing, where the cell attempts to maintain mitochondrial quality control and autophagic flux under compromised conditions. The decrease in *Map1lc3*, *Bnip3*, and *P62* suggests an initial impairment in the autophagic and mitophagic processes.<sup>87</sup> However, the upregulation of *Parkin*, *Optn*, and *Ndp52* may be a compensatory response to enhance the recognition and clearance of damaged mitochondria. For instance, considering that p62 recognizes and binds ubiquitinated cargo (such as damaged mitochondria tagged by PARKIN) and brings it to the autophagosome for degradation, the downregulation of P62 could impair the clearance of these damaged mitochondria, even if PARKIN is upregulated.<sup>90,91</sup> Therefore, despite the upregulation of PARKIN, there may still be issues in the overall mitophagy process due to insufficient P62.

ARC is an important nucleus that is not only involved in metabolic homeostasis and reproduction but also in behavioral regulation via its connections with other brain regions.<sup>92</sup> Activation of AgRP neurons was found to reduce anxiety-like behaviors<sup>93,94</sup> as well as locomotor activity.<sup>95</sup> Conversely, previous studies reported that POMC neuron activity<sup>46,96,97</sup> and *Pomc* mRNA levels in the ARC were elevated in response to the stress conditions<sup>98–100</sup> and ablation of POMC neurons in the ARC decreased locomotor activity.<sup>43</sup> In our study, even though not significantly, total distance traveled and mean velocity were reduced in both behavioral tests for the rotenone-administered group, indicating decreased locomotor activity in these animals. On the other hand, while rotenone-administered animals tended to exhibit anxiety-like behaviors as observed in the EPM test, they spent longer time in the center area in the OFT, suggesting reduced anxiety. The reason for the longer time spent in the center may be attributed to the reduced locomotion and mobility of the animals during OFT, rather than reduced anxiety. On the other hand, when considering the elevated *Pomc* mRNA levels, as well as reduced AgRP neuron activity, in *Fam163a* KD animals, it was expected to observe increased anxiety-like behaviors and locomotor activity. However, our results showed that *Fam163a* KD in the ARC did not alter locomotor activity and anxiety-like behaviors significantly, while nearly significantly increased elevation in the time spent in the center area in the OFT was observed. This can be attributed to the complex neuronal signaling between different neuronal populations in the ARC, including the circuits between AgRP and POMC neurons<sup>101</sup> and other connections with other nuclei in the brain.<sup>102,103</sup>

Hypothalamic mitochondrial dynamics play a role in energy homeostasis by regulating the neuronal activity of AgRP and POMC neurons.<sup>20,21</sup> Leptin, an adipose-derived hormone, is crucial for the regulation of food intake and

energy balance<sup>104</sup> and activates and inhibits the activity of POMC and AgRP neurons, respectively.<sup>105</sup> Previously, it was reported that activation of AgRP neurons potentiates lipogenesis in the white adipose tissue<sup>106</sup> and serum leptin levels are significantly correlated with body fat amount.<sup>107</sup> On the other hand, the International Mouse Phenotyping Consortium reported that full body *Fam163a* knockout mice exhibited significantly lower total body fat and significantly higher lean body mass with no alterations in total body weight.<sup>108,109</sup> Although the total fat amount of the animals in our study was not evaluated, reduced levels of leptin levels together with declined firing rates of AgRP neurons in *Fam163a* KD animals suggest that hypothalamic FAM163A may regulate serum leptin levels through its actions on the activities of hypothalamic hunger and satiety neurons. In addition, activities of the POMC and AgRP neurons are strongly connected with mitochondrial dynamics and function.<sup>20,23,59,110</sup> Considering the changes in mitochondria and redox-related gene expression in our study, the reduction in AgRP neuron firing frequency resulting from both *Fam163a* silencing and rotenone administration suggests that the activity of AgRP neurons may be influenced by mitochondrial mechanisms.

While our study provides significant insights into the role of FAM163A in hypothalamic neuronal activity and mitochondrial dynamics, several limitations should be acknowledged. We used an shRNA-based approach for the *Fam163a* knockdown in the ARC. While this method effectively reduced gene and protein expression levels in the ARC and diminished the AgRP neuron activity, the lack of cell-type specificity should be noted. Further studies employing Cre-dependent knockdown vectors or cell-type specific knockout models would provide greater specificity and validate the findings. Second, the activities of other neuronal populations, such as POMC neurons, following *Fam163a* silencing and mitochondrial stress were not investigated. Assessing the mitochondrial dynamics and neuronal activity of these neurons would provide a more comprehensive understanding of the interplay between these critical hypothalamic populations. Moreover, while qRT-PCR and immunofluorescence provided valuable insights into FAM163A expression in the hypothalamus, complementary quantitative alternative methods, such as Western blotting or mass spectrometry, could enhance accuracy and offer a broader analysis of FAM163A expression. Moreover, the findings regarding mitochondrial alterations following *Fam163a* knockdown and rotenone treatment are primarily based on gene expression analyses. Direct assessments of mitochondrial morphology and function using advanced techniques, such as transmission electron microscopy (TEM) for structural changes, high-resolution respirometry for mitochondrial respiration, and live-cell imaging for real-time mitochondrial dynamics,

would further elucidate the mitochondrial changes underlying the observed effects on neuronal activity.

## 4 | MATERIALS AND METHODS

### 4.1 | Animal husbandry

A total of 28 wild-type male C57BL/6 mice and 16 transgenic male *Agrp-ires-cre* (*Agrp*<sup>tm1(cre)Lowl</sup>, Jackson Labs Stock no: #012899) mice were used. All animals were housed under controlled conditions (temperature:  $21.0 \pm 1.0^\circ\text{C}$ , light/dark cycle: 12 h/12 h) having ad libitum access to standard chow food and water.<sup>111</sup> General health of the animals was monitored daily, and abnormalities (if any) were reported to the responsible veterinarian of the facility.

### 4.2 | Stereotaxic surgeries

Stereotaxic surgeries were performed as described previously.<sup>112,113</sup> Briefly, mice (P42–P52) were anesthetized with isoflurane (1.5%–2.0%) in the stereotaxic instrument (David Kopf Instruments, Tujunga, CA, USA). Following a 1 cm long scalp incision, the skull was drilled to create a tiny injection hole using a dental drill (1.4 mm diameter). Intracranial injections of 300–400 nL of virus or 200 nL of chemicals were performed bilaterally on the ARC region (posterior: 1.38 mm, lateral:  $\pm 0.38$  mm, and vertical: 5.82 mm) using a pulled glass pipette (Drummond Scientific, Wiretrol, Broomall-PA) with a tip diameter of 50  $\mu\text{m}$ , at a rate of 40 nL/min by a micromanipulator (Narishige, East Meadow, NY, USA), allowing 10 min for each injection. After removing the pipette, the surgical area was washed with Ringer's solution, the scalp was sutured with 5.0 silk surgical sutures, and cleaned with povidone-iodine for antisepsis. The animals were given at least a 2–3 weeks recovery period after the injections before doing additional tests. After the recovery period, the animals were divided into cages according to their experimental groups.

### 4.3 | Experimental groups

The study was divided into two different experimental sets in line with its aims (to investigate the effects of *Fam163a* silencing and mitochondrial dysfunction in the ARC). The first pair of groups included the control shRNA- and the *Fam163a* shRNA-administered (*Fam163a* KD) groups. The second two groups consisted of rotenone and its solvent, dimethyl sulfoxide (DMSO) groups.

The wild-type male C57BL/6 and *Agrp-ires-cre* mice were divided into four groups: DMSO group, rotenone

group, control shRNA-administered group (Neg. Ctr.), and *Fam163a* KD group, with 7 C57BL/6 and 4 *Agrp-ires-cre* mice in each group. Mice in the DMSO group received intracranial injections of DMSO as the vehicle (Sigma, D8418), while those in the rotenone group received 50 mM (1.97  $\mu\text{g}/\text{site}$ ) rotenone (Cayman Chemical Company, 13995) dissolved in DMSO intracranially.<sup>112</sup> Mice in the Neg. Ctr. group received intracranial injections of control shRNA lentiviral particles (Santa Cruz Biotechnology, sc-108080), while those in the *Fam163a* KD group received intracranial injections of *Fam163a* shRNA (m) lentiviral particles (Santa Cruz Biotechnology, sc-140624-V). Each *Agrp-ires-cre* mouse also received an injection of AAV pCAG-FLEX-EGFP-WPRE (AddGene, 51502-AAV9) to label AgRP neurons for electrophysiological recordings.<sup>113,114</sup>

### 4.4 | Behavioral studies

#### 4.4.1 | Food intake and body weight measurements

After a recovery period of 2 weeks, the wild-type animals were individually housed and allowed to habituate for 3–4 days with ad libitum access to standard chow and water. After habituation, animals were monitored for 25 days. Animals' feeding behavior was assessed at 24-h intervals. The amount of food consumption and body weight measurements were taken every day and every other day, respectively, at 10:00–11:00 a.m.

#### 4.4.2 | Open field test

The open field test (OFT) is widely used to assess the locomotor activity and anxiety-like behaviors of rodents.<sup>115,116</sup> After the food intake and body weight measurements, mice were subjected to OFT. All mice were habituated in the test room for an hour. The animals were then placed in an open field chamber (length  $\times$  width  $\times$  height = 80 cm  $\times$  80 cm  $\times$  50 cm), and their activities were recorded for 10 min by a camera. The time spent in the central and peripheral areas, the total distance traveled, and the speed were analyzed using the Ethovision XT 15 (Noldus) system. The arena was cleaned with 70% ethanol before each new animal was tested.

#### 4.4.3 | Elevated plus maze test

The elevated plus maze (EPM) test is used to evaluate anxiety-like behaviors in rodents.<sup>117,118</sup> After the habituation of the animals in the test room for an hour, the

animals were placed in the center of the polypropylene maze with two open arms (length  $\times$  width = 50 cm  $\times$  10 cm) and two closed arms (length  $\times$  width  $\times$  height = 50 cm  $\times$  10 cm  $\times$  10 cm) facing forward to the open arm of the polypropylene maze that was elevated for 50 cm. Their activities were monitored by a camera for 5 min. The time spent in the open and closed arms, the number of entries into the arms, the total distance traveled, and the average speed were analyzed using the Ethovision XT 15 (Noldus) system. The maze was cleaned with 70% ethanol before each new animal was tested.

#### 4.5 | Determination of blood glucose and serum insulin and leptin levels

Blood was collected from wild-type animals via cardiac puncture during sacrifice. Blood glucose levels were measured using a glucometer (Vivachek Eco). Serum samples obtained from the blood were stored at  $-80^{\circ}\text{C}$  until the measurements. Serum insulin levels and leptin levels were measured using the Mercodia Ultrasensitive Mouse Insulin ELISA kit (Mercodia, 10-1249-01) and Mouse LEP (Leptin) ELISA Kit (Elabscience, E-EL-M3008), respectively, according to the manufacturer's instructions.

#### 4.6 | RNA isolation, cDNA synthesis, and gene expression analyses

After the blood collection, animals were transcardially perfused with 0.9% NaCl solution under isoflurane anesthesia, followed by brain dissection. Brain slices containing the hypothalamus at a thickness of 250  $\mu\text{m}$  were obtained using a vibrotome (Campden Instruments, 5100 mz). Samples of ARC regions were dissected with a micro punch and transferred into the microfuge tubes containing TRI reagent, homogenized by using a Bullet Blender X24 (NextAdvance) and RNA was isolated according to the manufacturer's instructions (DirectZol<sup>TM</sup> RNA MiniPrep Plus, Zymo Research, R2072). During the isolation of the RNA, samples were treated with DNase in order to eliminate genomic DNA from the samples according to manufacturer's instructions (DirectZol<sup>TM</sup> RNA MiniPrep Plus, Zymo Research, R2072). Total RNA was quantified, and cDNA was synthesized by using the reverse transcription kit including a blend of random primers and oligo(dT) and equal amounts of RNA (50–100 ng) according to the manufacturer's instructions (iScript<sup>TM</sup> cDNA Synthesis Kit, Bio-Rad, 1708891).

Primers for target transcripts related to mitochondrial biogenesis (*peroxisome proliferator-activated receptor gamma coactivator 1-alpha* [*Pgc-1a*], *peroxisome*

*proliferator-activated receptor gamma coactivator 1-beta* [*Pgc-1b*], *estrogen related receptor alpha* [*Erra*], *mitochondrial transcription factor A* [*Tfam*], nuclear respiratory factor 1 [*Nrf1*], and *nuclear respiratory factor 2* [*Nrf2*]), mitochondrial fusion (*Optic atrophy 1* [*Opa1*], mitofusin 1 [*Mfn1*], and mitofusin 2 [*Mfn2*]), mitophagy (*BCL2/adrenovirus E1B 19kDa protein-interacting protein 3* [*Bnip3*], nuclear dot protein 52 kDa [*Ndp52*], *optineurin* [*Optn*], *FUN14 domain containing 1* [*Fundc1*], *microtubule-associated protein 1A/1B light chain 3A* [*Map1lc3a* (*LC3*)], *Parkin*, *PTEN-induced kinase 1* (*Pink1*), and *P62* (*sequestosome 1* [*Sqstm1*]), oxidative stress (*uncoupling protein 2* [*Ucp2*], *Kelch-like ECH-associated protein 1* [*Keap1*], *heme oxygenase 1* [*Ho-1*], and *hypoxia-inducible factor 1-alpha* [*Hif-1a*], appetite (*Agrp* and *Pomc*), and the reference transcript (*beta-actin* [*B-Actin*]) were amplified by qRT-PCR using specific primers (Table S1) that were designed by using the online primer design tool Primer3web version 4.1.0 (<https://primer3.ut.ee/>).

Sequences were amplified by qRT-PCR using SsoAdvanced Universal SYBR Green Supermix<sup>TM</sup> on an InstaQ96 Plus device (HiMedia). The absence of primer dimers was confirmed, and a single distinct peak was observed in the melting curve analysis for each primer. Thermal cycle sequences are given in Table S2. Changes in gene expression were calculated using the  $2^{-\Delta\Delta\text{Ct}}$  method and expressed as fold changes relative to the respective control groups.

#### 4.7 | Confocal microscopy

After transcardiac perfusion with 0.9% NaCl solution, animals were transcardially perfused with 4% paraformaldehyde (PFA), and whole brain tissue was dissected and fixed in 4% PFA for 1 week. Brain sections with a thickness of 50  $\mu\text{m}$  were obtained using a vibrotome (Campden Instruments, 5100 mz) and incubated in phosphate-buffered saline (PBS, pH =  $7.3 \pm 0.2$ ) at  $4^{\circ}\text{C}$  for 24 h. The sections were then stained by immunofluorescence staining using a free-floating approach. Basically, sections were washed with PBS ( $3 \times 10$  min) and incubated in PBS with 0.5 M glycine for 45 min at room temperature. Sections were then permeabilized in PBS supplemented with 0.1% Triton X-100 for 1 h at  $4^{\circ}\text{C}$  and blocked in PBS containing 3% bovine serum albumin (BSA) and 0.05% Triton X-100 for 1 h at room temperature. After blocking, the sections were incubated with anti-FAM163A antibody (1:200, Santa Cruz Biotechnology, Clone: G-12, sc-393821) diluted in antibody dilution buffer (PBS containing 1% BSA and 0.05% Triton X-100) overnight at  $4^{\circ}\text{C}$ . After incubation, sections were washed with PBS ( $3 \times 10$  min) and incubated in secondary antibody (1:2000, Cell Signaling



Technology®, #8890) for 1 h at room temperature. After three further washes with PBS for 10 min, sections were coverslipped with mounting medium (Fluoroshield™ with DAPI; Sigma, F6057) and visualized under a confocal microscope (Zeiss, Axio Imager 2) equipped with appropriate lasers and filters. Protein expressions in the hypothalamus were analyzed using Fiji software.<sup>119</sup>

#### 4.8 | Electrophysiology

The electrophysiological recordings were obtained between 10.00 a.m. and 01.00 p.m., and the animals had ad libitum access to the standard chow food and water at least for 2 days prior to the electrophysiology experiments.<sup>7</sup> *AgRP-ires-Cre* mice were subjected to transcardiac perfusion with cold cutting solution (92 mM NMDG, 2.5 mM KCl, 1.25 mM NaH<sub>2</sub>PO<sub>4</sub>, 30 mM NaHCO<sub>3</sub>, 20 mM HEPES, 25 mM Glucose, 2 mM Thiourea, 5 mM Na-ascorbate, 3 mM Na-pyruvate, 0.5 mM CaCl<sub>2</sub>·2H<sub>2</sub>O, and 10 mM MgSO<sub>4</sub>·7H<sub>2</sub>O) under anesthesia, followed by brain dissection. The brains were then immersed in a 95% O<sub>2</sub>/5% CO<sub>2</sub> aerated ice-cold cutting solution, and 250-μm-thick fresh slices containing the hypothalamus were obtained with a vibrotome and transferred to 95% O<sub>2</sub>/5% CO<sub>2</sub> aerated artificial cerebrospinal fluid (aCSF) incubation solution (92 mM NaCl, 2.5 mM KCl, 1.25 mM NaH<sub>2</sub>PO<sub>4</sub>, 30 mM NaHCO<sub>3</sub>, 20 mM HEPES, 25 mM Glucose, 2 mM Thiourea, 5 mM Na-ascorbate, 3 mM Na-pyruvate, 2 mM CaCl<sub>2</sub>·2H<sub>2</sub>O, and 2 mM MgSO<sub>4</sub>·7H<sub>2</sub>O). The sections were incubated in this solution for at least 1 h at room temperature and transferred to the recording chamber containing recording aCSF solution (124 mM NaCl, 2.5 mM KCl, 1.25 mM NaH<sub>2</sub>PO<sub>4</sub>, 24 mM NaHCO<sub>3</sub>, 12.5 mM glucose, 5 mM HEPES, 2 mM CaCl<sub>2</sub>·2H<sub>2</sub>O, and 2 mM MgSO<sub>4</sub>·7H<sub>2</sub>O). Cell-attached loose-seal recordings were performed in voltage clamp mode, and action currents were recorded from GFP-expressing ARC<sup>AgRP</sup> neurons using electrodes with 4–5 MΩ tip resistances. Recording aCSF solution was used in the pipette while performing loose-seal recordings. MultiClamp 700B Amplifier (Molecular Devices, San Jose, CA) and Axon™ pCLAMP™ 11.3 software (Molecular Devices, San Jose, CA) were used to obtain and analyze data.

#### 4.9 | Statistical analysis

Statistical analyses were conducted using GraphPad Prism software (GraphPad Software, USA). Data were expressed as mean ± standard deviation. The normality of data distribution was examined using the Shapiro–Wilk

test. Outlier analysis was performed using the ROUT method ( $Q=1\%$ ).<sup>120</sup> Data with a normal distribution were compared using either Student's *t*-test, multiple *t*-test, or two-way ANOVA followed by Bonferroni's multiple comparison, while nonnormally distributed data were analyzed using the Mann–Whitney *U* test. All data were presented as mean ± standard deviation.  $p < 0.05$  was considered statistically significant.

### 5 | CONCLUSION

Our results suggest that the hypothalamic FAM163A may play a role in the regulation of the AgRP neuronal activity by influencing the expression of the genes related to mitochondrial dynamics and biogenesis and redox state. Moreover, although both *Fam163a* knockdown and rotenone reduced the activity of the AgRP neurons, their effects on the local bioenergetics and redox homeostasis likely operate through different mechanisms, which require further elucidation. Given that the hypothalamus contains various neuronal populations and circuits involved in regulating food intake, it is not possible to attribute the effects of these manipulations solely to the AgRP neuronal activity, and more comprehensive studies investigating the activities of other neurons, including POMC neurons, are required. Moreover, the deletion of *Fam163a* in particular neuronal populations within the ARC that regulate satiety and hunger could provide more definitive evidence regarding the effects of FAM163A in cellular and organismal metabolism. Nonetheless, our findings offer insight into the role of FAM163A and mitochondrial stress in the central regulation of metabolism.

#### AUTHOR CONTRIBUTIONS

**Cihan Suleyman Erdogan:** Conceptualization; methodology; validation; formal analysis; investigation; writing – original draft; writing – review and editing; visualization. **Yavuz Yavuz:** Conceptualization; methodology; validation; formal analysis; investigation; visualization. **Huseyin Bugra Ozgun:** Methodology; validation; formal analysis; investigation; visualization. **Volkan Adem Bilgin:** Methodology; validation; formal analysis; investigation; visualization. **Sami Agus:** Methodology. **Ugur Faruk Kalkan:** Investigation. **Bayram Yilmaz:** Conceptualization; resources; writing – original draft; writing – review and editing; visualization; funding acquisition; supervision.

#### ACKNOWLEDGMENTS

The graphical abstract is created with [BioRender.com](https://BioRender.com).

## FUNDING INFORMATION

This study was funded by the Yeditepe University Research Projects and Scientific Activities Support Commission (Project No: HD22006).

## CONFLICT OF INTEREST STATEMENT

The authors declare no conflicts of interest.

## DATA AVAILABILITY STATEMENT

The data that support the findings of this study are available from the corresponding author upon reasonable request.

## ORCID

Sami Agus  <https://orcid.org/0000-0002-3454-2348>

Bayram Yilmaz  <https://orcid.org/0000-0002-2674-6535>

## REFERENCES

- Myers MG Jr, Olson DP. Central nervous system control of metabolism. *Nature*. 2012;491(7424):357-363.
- Liu Z, Xiao T, Liu H. Leptin signaling and its central role in energy homeostasis. *Front Neurosci*. 2023;17:1238528.
- Roh E, Song DK, Kim MS. Emerging role of the brain in the homeostatic regulation of energy and glucose metabolism. *Exp Mol Med*. 2016;48(3):e216.
- Andermann ML, Lowell BB. Toward a wiring diagram understanding of appetite control. *Neuron*. 2017;95(4):757-778.
- Rau AR, Hentges ST. The relevance of AgRP neuron-derived GABA inputs to POMC neurons differs for spontaneous and evoked release. *J Neurosci*. 2017;37(31):7362-7372.
- Dicken MS, Hughes AR, Hentges ST. Gad1 mRNA as a reliable indicator of altered GABA release from orexigenic neurons in the hypothalamus. *Eur J Neurosci*. 2015;42(9):2644-2653.
- Sayar-Atasoy N, Aklan I, Yavuz Y, et al. AgRP neurons encode circadian feeding time. *Nat Neurosci*. 2024;27(1):102-115.
- Başer Ö, Yavuz Y, Özen D, et al. Effects of chronic high fat diet on mediobasal hypothalamic satiety neuron function in POMC-Cre mice. *Mol Metab*. 2024;82:101904.
- Tekin S, Erden Y, Sandal S, et al. Effects of apelin on reproductive functions: relationship with feeding behavior and energy metabolism. *Arch Physiol Biochem*. 2017;123(1):9-15.
- Cowley MA, Smart JL, Rubinstein M, et al. Leptin activates anorexigenic POMC neurons through a neural network in the arcuate nucleus. *Nature*. 2001;411(6836):480-484.
- Schwartz MW, Sipols AJ, Marks JL, et al. Inhibition of hypothalamic neuropeptide Y gene expression by insulin. *Endocrinology*. 1992;130(6):3608-3616.
- Sipols AJ, Baskin DG, Schwartz MW. Effect of intracerebroventricular insulin infusion on diabetic hyperphagia and hypothalamic neuropeptide gene expression. *Diabetes*. 1995;44(2):147-151.
- Benoit SC, Air EL, Coolen LM, et al. The catabolic action of insulin in the brain is mediated by melanocortins. *J Neurosci*. 2002;22(20):9048-9052.
- Secher A, Jelsing J, Baquero AF, et al. The arcuate nucleus mediates GLP-1 receptor agonist liraglutide-dependent weight loss. *J Clin Invest*. 2014;124(10):4473-4488.
- Meeran K, O'Shea D, Edwards CM, et al. Repeated intracerebroventricular administration of glucagon-like peptide-1-(7-36) amide or exendin-(9-39) alters body weight in the rat. *Endocrinology*. 1999;140(1):244-250.
- Chen W, Zhao H, Li Y. Mitochondrial dynamics in health and disease: mechanisms and potential targets. *Signal Transduct Target Ther*. 2023;8(1):333.
- Clemente-Suárez VJ, Redondo-Flórez L, Beltrán-Velasco AI, et al. Mitochondria and brain disease: a comprehensive review of pathological mechanisms and therapeutic opportunities. *Biomedicine*. 2023;11(9):2488.
- Khacho M, Slack RS. Mitochondrial dynamics in the regulation of neurogenesis: from development to the adult brain. *Dev Dyn*. 2018;247(1):47-53.
- Rangaraju V, Lewis TL Jr, Hirabayashi Y, et al. Pleiotropic mitochondria: the influence of mitochondria on neuronal development and disease. *J Neurosci*. 2019;39(42):8200-8208.
- Dietrich MO, Liu ZW, Horvath TL. Mitochondrial dynamics controlled by mitofusins regulate AgRP neuronal activity and diet-induced obesity. *Cell*. 2013;155(1):188-199.
- Schneeberger M, Dietrich MO, Sebastián D, et al. Mitofusin 2 in POMC neurons connects ER stress with leptin resistance and energy imbalance. *Cell*. 2013;155(1):172-187.
- Andrews ZB, Liu ZW, Wallingford N, et al. UCP2 mediates ghrelin's action on NPY/AgRP neurons by lowering free radicals. *Nature*. 2008;454(7206):846-851.
- Diano S, Liu ZW, Jeong JK, et al. Peroxisome proliferation-associated control of reactive oxygen species sets melanocortin tone and feeding in diet-induced obesity. *Nat Med*. 2011;17(9):1121-1127.
- Li N, Ragheb K, Lawler G, et al. Mitochondrial complex I inhibitor rotenone induces apoptosis through enhancing mitochondrial reactive oxygen species production. *J Biol Chem*. 2003;278(10):8516-8525.
- Rochford JJ, Myers MG Jr, Heisler LK. Setting the tone: reactive oxygen species and the control of appetitive melanocortin neurons. *Cell Metab*. 2011;14(5):573-574.
- Minakhina S, Kim SY, Wondisford FE. Regulation of hypothalamic reactive oxygen species and feeding behavior by phosphorylation of the beta 2 thyroid hormone receptor isoform. *Sci Rep*. 2024;14(1):7200.
- Vasudevan SA, Shang X, Chang S, et al. Neuroblastoma-derived secretory protein is a novel secreted factor overexpressed in neuroblastoma. *Mol Cancer Ther*. 2009;8(8):2478-2489.
- Miwa H, Itoh N. Unknown genes, Cebelin and Cebelin-like, predominantly expressed in mouse brain. *Heliyon*. 2018;4(9):e00773.
- Qiao GJ, Chen L, Wu JC, Li ZR. Identification of an eight-gene signature for survival prediction for patients with hepatocellular carcinoma based on integrated bioinformatics analysis. *PeerJ*. 2019;7:e6548.
- Prados J, Stenz L, Courtet P, et al. Borderline personality disorder and childhood maltreatment: a genome-wide methylation analysis. *Genes Brain Behav*. 2015;14(2):177-188.
- Kober P, Boresowicz J, Rusetska N, et al. The role of aberrant DNA methylation in misregulation of gene expression in gonadotroph nonfunctioning pituitary tumors. *Cancer*. 2019;11(11):1650.
- Tsai TS, Tyagi S, St John JC. The molecular characterisation of mitochondrial DNA deficient oocytes using a pig model. *Hum Reprod (Oxford)*. 2018;33(5):942-953.

33. Ronci M, Pieroni L, Greco V, et al. Sequential fractionation strategy identifies three missing proteins in the mitochondrial proteome of commonly used cell lines. *J Proteome Res.* 2018;17(12):4307-4314.
34. Liu N, Zhou H, Zhang X, et al. FAM163A, a positive regulator of ERK signaling pathway, interacts with 14-3-3 $\beta$  and promotes cell proliferation in squamous cell lung carcinoma. *Onco Targets Ther.* 2019;12:6393-6406.
35. Chen YL, Li XL, Li G, et al. BRD4 inhibitor GNE987 exerts anti-cancer effects by targeting super-enhancers in neuroblastoma. *Cell Biosci.* 2022;12(1):33.
36. Sunkin SM, Ng L, Lau C, et al. Allen brain atlas: an integrated spatio-temporal portal for exploring the central nervous system. *Nucleic Acids Res.* 2013;41(Database issue):D996-D1008.
37. Lein ES, Hawrylycz MJ, Ao N, et al. Genome-wide atlas of gene expression in the adult mouse brain. *Nature.* 2007;445(7124):168-176.
38. Bonthuis PJ, Huang WC, Stacher Hörndli CN, Ferris E, Cheng T, Gregg C. Noncanonical genomic imprinting effects in offspring. *Cell Rep.* 2015;12(6):979-991.
39. Ruud J, Steculorum SM, Brüning JC. Neuronal control of peripheral insulin sensitivity and glucose metabolism. *Nat Commun.* 2017;8:15259.
40. Korgan AC, Oliveira-Abreu K, Wei W, et al. High sucrose consumption decouples intrinsic and synaptic excitability of AgRP neurons without altering body weight. *Int J Obes Lond.* 2023;47(3):224-235.
41. Caron A, Dungan Lemko HM, Castorena CM, et al. POMC neurons expressing leptin receptors coordinate metabolic responses to fasting via suppression of leptin levels. *elife.* 2018;7:7.
42. Mesaros A, Koralov SB, Rother E, et al. Activation of Stat3 signaling in AgRP neurons promotes locomotor activity. *Cell Metab.* 2008;7(3):236-248.
43. Zhan C, Zhou J, Feng Q, et al. Acute and long-term suppression of feeding behavior by POMC neurons in the brainstem and hypothalamus, respectively. *J Neurosci.* 2013;33(8):3624-3632.
44. Huo L, Gamber K, Greeley S, et al. Leptin-dependent control of glucose balance and locomotor activity by POMC neurons. *Cell Metab.* 2009;9(6):537-547.
45. Fang X, Jiang S, Wang J, et al. Chronic unpredictable stress induces depression-related behaviors by suppressing AgRP neuron activity. *Mol Psychiatry.* 2021;26(6):2299-2315.
46. Fang X, Chen Y, Wang J, et al. Increased intrinsic and synaptic excitability of hypothalamic POMC neurons underlies chronic stress-induced behavioral deficits. *Mol Psychiatry.* 2023;28(3):1365-1382.
47. Guo Z, Ruan Z, Zhang D, Liu X, Hou L, Wang Q. Rotenone impairs learning and memory in mice through microglia-mediated blood brain barrier disruption and neuronal apoptosis. *Chemosphere.* 2022;291(Pt 2):132982.
48. Sherer TB, Betarbet R, Testa CM, et al. Mechanism of toxicity in rotenone models of Parkinson's disease. *J Neurosci.* 2003;23(34):10756-10764.
49. Chaturvedi RK, Calingasan NY, Yang L, Hennessey T, Johri A, Beal MF. Impairment of PGC-1 $\alpha$  expression, neuropathology and hepatic steatosis in a transgenic mouse model of Huntington's disease following chronic energy deprivation. *Hum Mol Genet.* 2010;19(16):3190-3205.
50. Li PA, Hou X, Hao S. Mitochondrial biogenesis in neurodegeneration. *J Neurosci Res.* 2017;95(10):2025-2029.
51. Sivalingam K, Cirino TJ, McLaughlin JP, Samikkannu T. HIV-tat and cocaine impact brain energy metabolism: redox modification and mitochondrial biogenesis influence NRF transcription-mediated neurodegeneration. *Mol Neurobiol.* 2021;58(2):490-504.
52. Gyengesi E, Paxinos G, Andrews ZB. Oxidative stress in the hypothalamus: the importance of calcium signaling and mitochondrial ROS in body weight regulation. *Curr Neuropharmacol.* 2012;10(4):344-353.
53. Kuo DY, Chen PN, Yang SF, et al. Role of reactive oxygen species-related enzymes in neuropeptide y and proopiomelanocortin-mediated appetite control: a study using atypical protein kinase C knockdown. *Antioxid Redox Signal.* 2011;15(8):2147-2159.
54. Cunarro J, Casado S, Lugalde J, Tovar S. Hypothalamic mitochondrial dysfunction as a target in obesity and metabolic disease. *Front Endocrinol.* 2018;9:283.
55. Jin S, Diano S. Mitochondrial dynamics and hypothalamic regulation of metabolism. *Endocrinology.* 2018;159(10):3596-3604.
56. Stastna M. Proteomics as a tool for the study of mitochondrial proteome, its dysfunctionality and pathological consequences in cardiovascular diseases. *Int J Mol Sci.* 2023;24(5):4692.
57. Haigh JL, New LE, Filippi BM. Mitochondrial dynamics in the brain are associated with feeding, glucose homeostasis, and whole-body metabolism. *Front Endocrinol Lausanne.* 2020;11:580879.
58. Zorzano A, Claret M. Implications of mitochondrial dynamics on neurodegeneration and on hypothalamic dysfunction. *Front Aging Neurosci.* 2015;7:101.
59. Ramírez S, Gómez-Valadés AG, Schneeberger M, et al. Mitochondrial dynamics mediated by Mitofusin 1 is required for POMC neuron glucose-sensing and insulin release control. *Cell Metab.* 2017;25(6):1390-1399.e1396.
60. Gómez-Valadés AG, Pozo M, Varela L, et al. Mitochondrial cristae-remodeling protein OPA1 in POMC neurons couples Ca(2+) homeostasis with adipose tissue lipolysis. *Cell Metab.* 2021;33(9):1820-1835.e1829.
61. Chen H, Detmer SA, Ewald AJ, Griffin EE, Fraser SE, Chan DC. Mitofusins Mfn1 and Mfn2 coordinately regulate mitochondrial fusion and are essential for embryonic development. *J Cell Biol.* 2003;160(2):189-200.
62. Scorrano L. Mitochondrial dynamics. In: Lennarz WJ, Lane MD, eds. *Encyclopedia of Biological Chemistry.* 2nd ed. Academic Press; 2013:135-139.
63. de Brito OM, Scorrano L. Mitofusin 2 tethers endoplasmic reticulum to mitochondria. *Nature.* 2008;456(7222):605-610.
64. Ozcan M, Alcín E, Ayar A, Yilmaz B, Sandal S, Kelestimur H. Kisspeptin-10 elicits triphasic cytosolic calcium responses in immortalized GT1-7 GnRH neurones. *Neurosci Lett.* 2011;492(1):55-58.
65. Scarpulla RC, Vega RB, Kelly DP. Transcriptional integration of mitochondrial biogenesis. *Trends Endocrinol Metab.* 2012;23(9):459-466.
66. Soriano FX, Liesa M, Bach D, Chan DC, Palacín M, Zorzano A. Evidence for a mitochondrial regulatory pathway defined by peroxisome proliferator-activated receptor- $\gamma$  coactivator-1  $\alpha$ , estrogen-related receptor- $\alpha$ , and mitofusin 2. *Diabetes.* 2006;55(6):1783-1791.
67. Peng K, Tao Y, Zhang J, et al. Resveratrol regulates mitochondrial biogenesis and fission/fusion to attenuate rotenone-induced neurotoxicity. *Oxidative Med Cell Longev.* 2016;2016:6705621.



68. Peng K, Yang L, Wang J, et al. The interaction of mitochondrial biogenesis and fission/fusion mediated by PGC-1 $\alpha$  regulates rotenone-induced dopaminergic neurotoxicity. *Mol Neurobiol*. 2017;54(5):3783-3797.
69. Hwang RD, Wiemerslage L, LaBreck CJ, et al. The neuroprotective effect of human uncoupling protein 2 (hUCP2) requires cAMP-dependent protein kinase in a toxin model of Parkinson's disease. *Neurobiol Dis*. 2014;69:180-191.
70. Youle RJ, van der Bliek AM. Mitochondrial fission, fusion, and stress. *Science*. 2012;337(6098):1062-1065.
71. Sidarala V, Zhu J, Levi-D'Ancona E, et al. Mitofusin 1 and 2 regulation of mitochondrial DNA content is a critical determinant of glucose homeostasis. *Nat Commun*. 2022;13(1):2340.
72. Zhang X, Du L, Zhang W, Yang Y, Zhou Q, Du G. Therapeutic effects of baicalein on rotenone-induced Parkinson's disease through protecting mitochondrial function and biogenesis. *Sci Rep*. 2017;7(1):9968.
73. Wang T, Li C, Han B, et al. Neuroprotective effects of Danshensu on rotenone-induced Parkinson's disease models in vitro and in vivo. *BMC Complement Med Ther*. 2020;20(1):20.
74. Johnson DA, Johnson JA. Nrf2—a therapeutic target for the treatment of neurodegenerative diseases. *Free Radic Biol Med*. 2015;88(Pt B):253-267.
75. Lou H, Jing X, Wei X, Shi H, Ren D, Zhang X. Naringenin protects against 6-OHDA-induced neurotoxicity via activation of the Nrf2/ARE signaling pathway. *Neuropharmacology*. 2014;79:380-388.
76. Lee S, Hu L. Nrf2 activation through the inhibition of Keap1-Nrf2 protein-protein interaction. *Med Chem Res*. 2020;29(5):846-867.
77. Moreira S, Fonseca I, Nunes MJ, et al. Nrf2 activation by tauroursodeoxycholic acid in experimental models of Parkinson's disease. *Exp Neurol*. 2017;295:77-87.
78. Baird L, Yamamoto M. The molecular mechanisms regulating the KEAP1-NRF2 pathway. *Mol Cell Biol*. 2020;40(13):e00099-20.
79. Liu S, Pi J, Zhang Q. Mathematical modeling reveals quantitative properties of KEAP1-NRF2 signaling. *Redox Biol*. 2021;47:102139.
80. Zhu S, Wu H, Cui H, et al. Induction of mitophagy via ROS-dependent pathway protects copper-induced hypothalamic nerve cell injury. *Food Chem Toxicol*. 2023;181:114097.
81. Morselli E, Criollo A, Rodriguez-Navas C, Clegg DJ. Chronic high fat diet consumption impairs metabolic health of male mice. *Inflamm Cell Signal*. 2014;1(6):e561.
82. Tanida I, Ueno T, Kominami E. LC3 conjugation system in mammalian autophagy. *Int J Biochem Cell Biol*. 2004;36(12):2503-2518.
83. Gonçalves FB, Morais VA. PINK1: a bridge between mitochondria and Parkinson's disease. *Life Basel*. 2021;11(5):371.
84. Ge P, Dawson VL, Dawson TM. PINK1 and Parkin mitochondrial quality control: a source of regional vulnerability in Parkinson's disease. *Mol Neurodegener*. 2020;15(1):20.
85. Truban D, Hou X, Caulfield TR, Fiesel FC, Springer W. PINK1, Parkin, and mitochondrial quality control: what can we learn about Parkinson's disease pathobiology? *J Parkinsons Dis*. 2017;7(1):13-29.
86. Wong YC, Holzbaur EL. Optineurin is an autophagy receptor for damaged mitochondria in parkin-mediated mitophagy that is disrupted by an ALS-linked mutation. *Proc Natl Acad Sci USA*. 2014;111(42):E4439-E4448.
87. Durcan TM, Fon EA. The three 'P's of mitophagy: PARKIN, PINK1, and post-translational modifications. *Genes Dev*. 2015;29(10):989-999.
88. Gustafsson ÅB, Dorn GW 2nd. Evolving and expanding the roles of mitophagy as a homeostatic and pathogenic process. *Physiol Rev*. 2019;99(1):853-892.
89. Li J, Lin Q, Shao X, et al. HIF1 $\alpha$ -BNIP3-mediated mitophagy protects against renal fibrosis by decreasing ROS and inhibiting activation of the NLRP3 inflammasome. *Cell Death Dis*. 2023;14(3):200.
90. Wurzer B, Zaffagnini G, Fracchiolla D, et al. Oligomerization of p62 allows for selection of ubiquitinated cargo and isolation membrane during selective autophagy. *elife*. 2015;4:e08941.
91. Narendra D, Kane LA, Hauser DN, Fearnley IM, Youle RJ. p62/SQSTM1 is required for Parkin-induced mitochondrial clustering but not mitophagy; VDAC1 is dispensable for both. *Autophagy*. 2010;6(8):1090-1106.
92. Leon-Mercado L, Herrera Moro Chao D, Basualdo MD, Kawata M, Escobar C, Buijs RM. The arcuate nucleus: a site of fast negative feedback for corticosterone secretion in male rats. *eNeuro*. 2017;4(1):ENEURO.0350-16.2017.
93. Dietrich MO, Zimmer MR, Bober J, Horvath TL. Hypothalamic AgRP neurons drive stereotypic behaviors beyond feeding. *Cell*. 2015;160(6):1222-1232.
94. Burnett CJ, Li C, Webber E, et al. Hunger-driven motivational state competition. *Neuron*. 2016;92(1):187-201.
95. Jiang J, Morgan DA, Cui H, Rahmouni K. Activation of hypothalamic AgRP and POMC neurons evokes disparate sympathetic and cardiovascular responses. *Am J Physiol Heart Circ Physiol*. 2020;319(5):H1069-H1077.
96. Liu J, Garza JC, Truong HV, Henschel J, Zhang W, Lu XY. The melanocortinergic pathway is rapidly recruited by emotional stress and contributes to stress-induced anorexia and anxiety-like behavior. *Endocrinology*. 2007;148(11):5531-5540.
97. Qu N, He Y, Wang C, et al. A POMC-originated circuit regulates stress-induced hypophagia, depression, and anhedonia. *Mol Psychiatry*. 2020;25(5):1006-1021.
98. Larsen PJ, Mau SE. Effect of acute stress on the expression of hypothalamic messenger ribonucleic acids encoding the endogenous opioid precursors preproenkephalin A and proopiomelanocortin. *Peptides*. 1994;15(5):783-790.
99. Baubet V, Fèvre-Montange M, Gay N, Debilly G, Bobillier P, Cespuoglio R. Effects of an acute immobilization stress upon proopiomelanocortin (POMC) mRNA levels in the mediobasal hypothalamus: a quantitative in situ hybridization study. *Brain Res Mol Brain Res*. 1994;26(1-2):163-168.
100. Yamano Y, Yoshioka M, Toda Y, et al. Regulation of CRF, POMC and MC4R gene expression after electrical foot shock stress in the rat amygdala and hypothalamus. *J Vet Med Sci*. 2004;66(11):1323-1327.
101. Jais A, Brüning JC. Arcuate nucleus-dependent regulation of metabolism-pathways to obesity and diabetes mellitus. *Endocr Rev*. 2022;43(2):314-328.
102. Haspula D, Cui Z. Neurochemical basis of inter-organ crosstalk in health and obesity: focus on the hypothalamus and the brainstem. *Cells*. 2023;12(13):1801. doi:10.3390/cells12131801
103. Wang D, He X, Zhao Z, et al. Whole-brain mapping of the direct inputs and axonal projections of POMC and AgRP neurons. *Front Neuroanat*. 2015;9:40. doi:10.3389/fnana.2015.00040



104. Timper K, Brüning JC. Hypothalamic circuits regulating appetite and energy homeostasis: pathways to obesity. *Dis Model Mech*. 2017;10(6):679-689.
105. Varela L, Horvath TL. Leptin and insulin pathways in POMC and AgRP neurons that modulate energy balance and glucose homeostasis. *EMBO Rep*. 2012;13(12):1079-1086.
106. Cavalcanti-de-Albuquerque JP, Bober J, Zimmer MR, Dietrich MO. Regulation of substrate utilization and adiposity by AgRP neurons. *Nat Commun*. 2019;10(1):311.
107. Considine RV, Sinha MK, Heiman ML, et al. Serum immunoreactive-leptin concentrations in normal-weight and obese humans. *N Engl J Med*. 1996;334(5):292-295.
108. Groza T, Gomez FL, Mashhadi HH, et al. The international mouse phenotyping consortium: comprehensive knockout phenotyping underpinning the study of human disease. *Nucleic Acids Res*. 2023;51(D1):D1038-D1045.
109. Informatics MG. Phenotype Data for MGI:3618859. <https://www.mousephenotype.org/data/genes/MGI:3618859>. Accessed June, 22, 2024
110. Jin S, Yoon NA, Liu ZW, et al. Drp1 is required for AgRP neuronal activity and feeding. *elife*. 2021;10:e64351.
111. Canpolat S, Tug N, Seyran AD, Kumru S, Yilmaz B. Effects of raloxifene and estradiol on bone turnover parameters in intact and ovariectomized rats. *J Physiol Biochem*. 2010;66(1):23-28.
112. Dilsiz P, Aklan I, Sayar Atasoy N, et al. MCH neuron activity is sufficient for reward and reinforces feeding. *Neuroendocrinology*. 2020;110(3-4):258-270.
113. Sayar-Atasoy N, Laule C, Aklan I, et al. Adrenergic modulation of melanocortin pathway by hunger signals. *Nat Commun*. 2023;14(1):6602.
114. Ates T, Oncul M, Dilsiz P, et al. Inactivation of Magel2 suppresses oxytocin neurons through synaptic excitation-inhibition imbalance. *Neurobiol Dis*. 2019;121:58-64.
115. Kraeuter AK, Guest PC, Sarnyai Z. The open field test for measuring locomotor activity and anxiety-like behavior. *Methods Mol Biol*. 2019;1916:99-103.
116. Yavuz Y, Ozen DO, Erol ZY, Goren H, Yilmaz B. Effects of endocrine disruptors on the electrical activity of leptin receptor neurons in the dorsomedial hypothalamus and anxiety-like behavior in male mice. *Environ Pollut*. 2023;324:121366.
117. Kraeuter AK, Guest PC, Sarnyai Z. The elevated plus maze test for measuring anxiety-like behavior in rodents. *Methods Mol Biol*. 2019;1916:69-74.
118. Yavuz Y, Yesilay G, Guvenc Tuna B, et al. Investigation of effects of transferrin-conjugated gold nanoparticles on hippocampal neuronal activity and anxiety behavior in mice. *Mol Cell Biochem*. 2023;478(8):1813-1824.
119. Schindelin J, Arganda-Carreras I, Frise E, et al. Fiji: an open-source platform for biological-image analysis. *Nat Methods*. 2012;9(7):676-682.
120. Motulsky HJ, Brown RE. Detecting outliers when fitting data with nonlinear regression—a new method based on robust nonlinear regression and the false discovery rate. *BMC Bioinformatics*. 2006;7:123.

## SUPPORTING INFORMATION

Additional supporting information can be found online in the Supporting Information section at the end of this article.

**How to cite this article:** Erdogan CS, Yavuz Y, Ozgun HB, et al. *Fam163a* knockdown and mitochondrial stress in the arcuate nucleus of hypothalamus reduce AgRP neuron activity and differentially regulate mitochondrial dynamics in mice. *Acta Physiol*. 2025;241:e70020. doi:[10.1111/apha.70020](https://doi.org/10.1111/apha.70020)